SmoothGNN: Smoothing-aware GNN for Unsupervised Node Anomaly Detection

Xiangyu Dong
The Chinese University of Hong Kong
Hong Kong, China
xydong@se.cuhk.edu.hk

Xingyi Zhang
Mohamed bin Zayed University of Artificial Intelligence
Abu Dhabi, United Arab Emirates
xingyi.zhang@mbzuai.ac.ae

Yanni Sun
City University of Hong Kong
Hong Kong, China
yannisun@cityu.edu.hk

Lei Chen
Huawei Noah's Ark Lab
Hong Kong, China
lc.leichen@huawei.com

Mingxuan Yuan
Huawei Noah's Ark Lab
Hong Kong, China
yuan.mingxuan@huawei.com

Sibo Wang*
The Chinese University of Hong Kong
Hong Kong, China
swang@se.cuhk.edu.hk

Abstract

The smoothing issue in graph learning leads to indistinguishable node representations, posing significant challenges for graph-related tasks. However, our experiments reveal that this problem can uncover underlying properties of node anomaly detection (NAD) that previous research has missed. We introduce Individual Smoothing Patterns (ISP) and Neighborhood Smoothing Patterns (NSP), which indicate that the representations of anomalous nodes are harder to smooth than those of normal ones. In addition, we explore the theoretical implications of these patterns, demonstrating the potential benefits of ISP and NSP for NAD tasks. Motivated by these findings, we propose SmoothGNN, a novel unsupervised NAD framework. First, we design a learning component to explicitly capture ISP for detecting node anomalies. Second, we design a spectral graph neural network to implicitly learn ISP to enhance detection. Third, we design an effective coefficient based on our findings that NSP can serve as coefficients for node representations, aiding in the identification of anomalous nodes. Furthermore, we devise a novel anomaly measure to calculate loss functions and anomalous scores for nodes, reflecting the properties of NAD using ISP and NSP. Extensive experiments on 9 real datasets show that SmoothGNN outperforms the best rival by an average of 14.66% in AUC and 7.28% in Average Precision, with 75x running time speedup, validating the effectiveness and efficiency of our framework. Our code is available at https://github.com/xydong127/SmoothGNN.

CCS Concepts

• **Computing methodologies → Anomaly detection**.

Keywords

Unsupervised Node Anomaly Detection, Smoothing Patterns

*Sibo Wang is the corresponding author.

ACM Reference Format:
Xiangyu Dong, Xingyi Zhang, Yanni Sun, Lei Chen, Mingxuan Yuan, and Sibo Wang. 2025. SmoothGNN: Smoothing-aware GNN for Unsupervised Node Anomaly Detection. In *Proceedings of the ACM Web Conference 2025 (WWW '25), April 28-May 2, 2025, Sydney, NSW, Australia.* ACM, New York, NY, USA, 12 pages. https://doi.org/10.1145/3696410.3714615

1 Introduction

Node anomaly detection (NAD) aims to identify nodes in a graph that exhibit anomalous patterns compared to the majority of nodes [1, 24]. As the widespread prevalence of graph data driven by advances in modern technologies over the past three decades, NAD has become a trending topic due to its crucial role in various real-world applications, such as fraud detection in financial networks [16], malicious reviews detection in social networks [25], and hotspot detection in chip manufacturing [32].

However, the complicated information and large scale of real-world graphs present challenges in effectively and efficiently detecting anomalous nodes, especially in unsupervised settings [9, 14, 23]. To address these challenges, various designs have been proposed for the unsupervised NAD task, such as shallow models [21, 28], reconstruction models [18, 31], self-supervised models [11–13, 27], and special models [4, 15, 17, 29]. However, these methods usually face effectiveness or efficiency issues in real-world deployment for NAD tasks. To be specific, shallow models have limited expressiveness due to the hand-crafted rules, reconstruction models and self-supervised models are unlikely to be used in real applications due to high computational complexity, and special models face the challenge of finding an effective identifier of NAD.

To address these limitations, we re-evaluate the propagation procedure of NAD tasks and find that the smoothing issue can provide potential advantages for detecting anomalies in graphs. Specifically, we design two novel measures: *Individual Smoothing Patterns (ISP)* and *Neighborhood Smoothing Patterns (NSP)*, to analyze the smoothing issue from different perspectives. For ISP, we calculate the average normalized distances between node representations at each propagation hop and the converged representations obtained after an infinite number of hops for both anomalous and normal nodes. For NSP, we calculate the average normalized similarities within the neighborhoods of anomalous and normal nodes, respectively. Notably, these two smoothing patterns exhibit distinct

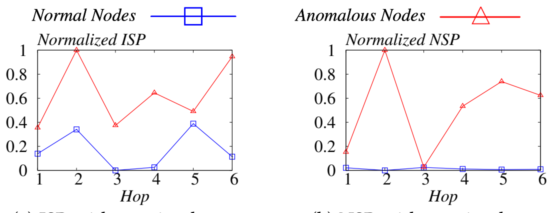

(a) ISP with varying hops (b) NSP with varying hops

Figure 1: Smoothing Patterns of Amazon.

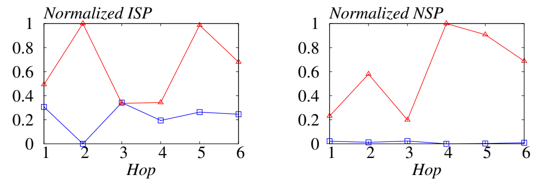

(a) ISP with varying hops (b) NSP with varying hops

Figure 2: Smoothing Patterns of T-Finance.

behaviors across different types of nodes in real-world datasets like Amazon and T-Finance, as illustrated in Figures 1 and 2, respectively. During propagation, the smoothing patterns of anomalous nodes generally exceed those of normal nodes at most hops. This observation provides a potential metric for assessing anomalous scores of nodes: the higher the smoothing patterns, the more likely a node is to be anomalous. Similar observations on other datasets can be found in Appendix A.2.

To explore the rationale behind this phenomenon, we conduct a theoretical analysis, revealing that the smoothing patterns are closely related to anomalous properties of nodes, originating from the structural and attribute information, as shown in Theorem 1. Besides, further exploration in Theorem 2 highlights the strong connection between the smoothing issue and the spectral space, providing insights for designing a spectral *Graph Neural Network (GNN)*. Moreover, as illustrated in Theorem 3, our findings indicate that NSP serves a role similar to spectral energy [8], which can be utilized as coefficients for node representations. Furthermore, we provide a theoretical guarantee in Theorem 4 to clarify the boundaries of the benefits derived from the smoothing issue.

Motivated by both experimental and theoretical findings, we introduce SmoothGNN, a novel graph learning framework for unsupervised NAD tasks. It consists of four key components: the *Smoothing-aware Learning Component (SLC)*, the *Smoothing-aware Spectral GNN (SSGNN)*, the *Smoothing-aware Coefficients (SC)*, and the *Smoothing-aware Measure (SMeasure)*. Specifically, SLC serves as a feature encoding module, explicitly capturing the ISP of anomalous and normal nodes, as supported by Theorem 1. Subsequently, based on Theorem 2, SSGNN is designed to learn node representations from the spectral space of the graph while implicitly capturing ISP to aid the learning process. Additionally, building upon Theorem 3, we design SC to extract both NSP and spectral energy information, providing complementary properties from other perspectives. Furthermore, through unifying the benefits of ISP and NSP proven by the empirical and theoretical results, we introduce a novel SMeasure to effectively and efficiently calculate the loss function and the anomalous scores. Ultimately, in contrast to previous studies in the unsupervised NAD area, such as [15, 29], which primarily focused on small or synthetic datasets, we conduct experiments on large-scale real datasets commonly encountered in practical applications, demonstrating the usefulness of SmoothGNN.

In summary, our work makes the following key contributions:

- To the best of our knowledge, we are the first to demonstrate the benefit of the smoothing issue on NAD tasks from both experimental and theoretical perspectives. Building upon this insight, we introduce a novel SMeasure as an anomaly measurement for unsupervised NAD tasks.
- We propose SmoothGNN, a novel framework that captures information from the smoothing process and spectral space of graphs, which can serve as a powerful backbone for NAD tasks.
- Our work stands out as the only one that conducts experiments on large real-world datasets for unsupervised NAD. Extensive experimental results showcase the effectiveness and efficiency of our proposed framework. Compared to state-of-the-art alternatives, SmoothGNN demonstrates superior performance in terms of AUC and Average Precision, with a speed-up of at least one order of magnitude.

2 Related Work

In recent years, unsupervised NAD has gained increasing interest within the graph learning community. Researchers have proposed a variety of models that can be broadly categorized into four groups: shallow models, reconstruction models, self-supervised models, and special models. Next, we briefly introduce several representative frameworks from these categories.

Shallow Models. Prior to the emergence of deep learning models, early works for the NAD tasks mainly focus on shallow models, which utilize statistical information and mathematical formulas to identify node anomalies. For instance, Radar [21] utilizes the residuals of attribute information and their coherence with graph information to identify anomalous nodes. ANOMALOUS [28] introduces a joint framework for NAD based on residual analysis. These models primarily adopt matrix decomposition and residual analysis, which inherently have limited capabilities in capturing the complex graph information, compared to deep learning models.

Reconstruction Models. Reconstruction models are prevalent approaches for unsupervised NAD, as the reconstruction errors of graph structures and node features inherently reflect the likelihood of a node being anomalous. Motivated by this, a prior work CLAD [18], proposes a label-aware reconstruction approach that utilizes Jensen-Shannon Divergence and Euclidean Distance. Besides, *graph auto-encoders (GAEs)* are widely adopted as reconstruction techniques. For example, GADNR [31] incorporates GAEs to reconstruct the neighborhood of nodes. Although previous studies have shown the usefulness of graph reconstruction, it is worth noting that reconstructing graph structures can be computationally expensive. Moreover, experimental findings [17] indicate that node feature reconstruction yields significant benefits for NAD. Therefore, a preferable choice is to focus exclusively on feature reconstruction to assist loss function, as introduced in the SmoothGNN framework.

Self-supervised Models. Aside from the reconstruction models, self-supervised models, such as contrastive learning frameworks, employ auxiliary tasks to guide unsupervised NAD. For example, NLGAD [13] constructs multi-scale contrastive learning networks to estimate the normality for nodes. Similarly, GRADATE [11] presents a multi-scale contrastive learning framework with subgraph-subgraph contrast to capture the local properties of nodes. Other examples include PREM [27] and ARISE [12], which employ node-subgraph contrast and node-node contrast to learn node representations, reflecting both local and global views of the graph. A recent study, TAM [29], leverages data augmentation to generate multi-view graphs, enabling the examination of the consistency of the local information within node neighborhoods. Based on the observation of local node affinity, TAM introduces a local affinity score to measure the probability of a node being anomalous, highlighting the importance of designing new measures for NAD. In contrast, SmoothGNN introduces the SMeasure to calculate anomalous scores, which utilizes a more flexible way to capture the anomalous properties of the nodes and requires fewer computational resources, enabling SmoothGNN to be applied to large-scale datasets.

Special Models. In addition to the above-mentioned models, there are also special models that leverage novel measurements to design loss or reward functions for calculating anomalous scores. For instance, RAND [4] is the first work that leverages reinforcement learning in the unsupervised NAD task. It introduces an anomaly-aware aggregator to amplify messages from reliable neighbors. On the other hand, VGOD [17] presents a mixed-type framework that combines a reconstruction model and a self-supervised model. It incorporates a variance-based module to sample positive and negative pairs for contrastive learning, along with an attribute reconstruction module to reconstruct node features. Afterward, REC [15] utilizes a score-based generative model to boost the performance in this area. In contrast to these works, our SmoothGNN framework adopts a different strategy with theoretical analyses by utilizing feature reconstruction and the proposed SMeasure as the objective function, which achieves superior performance while requiring significantly less running time.

3 Preliminaries

Notation. Let $G = (\boldsymbol{A}, \boldsymbol{X})$ denote a connected undirected graph with n nodes and m edges, where $\boldsymbol{X} \in \mathbb{R}^{n\times F}$ represents node features and $\boldsymbol{A} \in \mathbb{R}^{n\times n}$ represents the adjacency matrix. Let $\boldsymbol{A}_{ij} = 1$ if there exists an edge between node i and j, otherwise $\boldsymbol{A}_{ij} = 0$. $\boldsymbol{D}$ denotes the degree matrix. The adjacency matrix $\tilde{\boldsymbol{A}}$ and degree matrix $\tilde{\boldsymbol{D}}$ of graph G with self-loops can be defined as $\tilde{\boldsymbol{A}} = \boldsymbol{A} + \boldsymbol{I_n}$ and $\tilde{\boldsymbol{D}} = \boldsymbol{D}+\boldsymbol{I_n}$, respectively, where $\boldsymbol{I}_n \in \mathbb{R}^{n\times n}$ is an identity matrix. The Laplacian matrix $\boldsymbol{L}$ is then defined as $\boldsymbol{L} = \boldsymbol{I_n} - \tilde{\boldsymbol{D}}^{-\frac{1}{2}}\tilde{\boldsymbol{A}}\tilde{\boldsymbol{D}}^{-\frac{1}{2}}$. It can also be decomposed by $\boldsymbol{L} = \boldsymbol{U}\boldsymbol{\Lambda}\boldsymbol{U}^T$, where $\boldsymbol{U} = (\boldsymbol{u}_1, \boldsymbol{u}_2, ..., \boldsymbol{u}_n)$ represents orthonormal eigenvectors and the corresponding eigenvalues are sorted in ascending order, i.e. $\lambda_1 \le ... \le \lambda_n$. Let $\boldsymbol{x} = (x_1, x_2, ..., x_n)^T \in \mathbb{R}^n$ be a signal on graph G, the graph convolution operation between a signal $\boldsymbol{x}$ and a graph filter $g_\theta(\cdot)$ is then defined as $g_\theta(\boldsymbol{L}) * \boldsymbol{x} = \boldsymbol{U}g_\theta(\Lambda)\boldsymbol{U}^T\boldsymbol{x}$, where the parameter $\theta \in \mathbb{R}^n$ is spectral filter coefficient vector.

Unsupervised Node Anomaly Detection. Let $\mathbf{V} = \{v_1, ..., v_n\}$ denotes the node set of graph G, then unsupervised NAD tasks aim to learn an anomaly scoring function $f : \mathbf{V} \longrightarrow \mathbb{R}$, such that $f(v_n) < f(v_a)$, for $\forall v_n \in \mathbf{V}_n$ and $\forall v_a \in \mathbf{V}_a$, where $\mathbf{V}_n$ and $\mathbf{V}_a$ represents the normal and anomalous node set separately. In addition, due to the nature of the anomalies, it is typically assumed that $|\mathbf{V}_n| \gg |\mathbf{V}_a|$. Moreover, since this work focuses on the unsupervised setting, the class labels of the nodes during training are not accessible. Under such circumstances, unsupervised NAD tasks require effective and efficient techniques to help the learning of the framework.

Spectral GNN. Graph convolution operations [7, 19] can be approximated by the T-th order polynomial of Laplacians:

$$\boldsymbol{U}g_\theta(\Lambda)\boldsymbol{U}^T\boldsymbol{x} \approx \boldsymbol{U}(\sum_{t=0}^{T}\theta_t\boldsymbol{\Lambda}^t)\boldsymbol{U}^T\boldsymbol{x} = (\sum_{t=0}^{T}\theta_t\boldsymbol{L}^t)\boldsymbol{x},$$

where $\theta \in \mathbb{R}^{T+1}$ corresponds to polynomial coefficients. In the following Section 4.1, the prevalent graph convolution operation is demonstrated to have a strong relation with graph smoothing patterns. This key insight motivates the design of SmoothGNN, which can capture information from graph spectral space and anomalous properties behind smoothing patterns.

Individual Smoothing Patterns. As presented in a previous study [36], the node representations finally converge to a stable state, making it challenging to distinguish between different nodes. However, as discussed in Section 1, the distances between node representations at each propagation hop and the converged representations obtained after an infinite number of hops exhibit different patterns for anomalous and normal nodes. Hence, ISP can be denoted as:

$$I(\boldsymbol{x}) = \left\|(\boldsymbol{P}^t - \boldsymbol{P}^\infty)\boldsymbol{x}\right\|_2^2,$$

where $\boldsymbol{P}^t$ is the propagation matrix after t hops of propagation, P^∞ is the converged state, and $\boldsymbol{x}$ is the graph signal. ISP effectively describes the smoothing patterns of each individual node during propagation, as indicated by its definition. Subsequent analyses in Section 4.1 illustrate the effectiveness of ISP in NAD tasks, which can capture both spectral information and smoothing patterns.

Neighborhood Smoothing Patterns. To describe the smoothing patterns from a different perspective, we adopt the concept of Dirichlet Energy [39] to define NSP as follows:

$$N(\boldsymbol{x}^t) = \sum_{i,j=1}^{n} a_{i,j}\left\|\frac{x_i^t}{\sqrt{d_i+1}} - \frac{x_j^t}{\sqrt{d_j+1}}\right\|_2^2,$$

where $a_{i,j}$ represents the (i, j)-th entry of the adjacency matrix $\tilde{\boldsymbol{A}}$, d_i is the degree of node i, and $\boldsymbol{x}^t = \boldsymbol{P}^t\boldsymbol{x}$. According to this definition, NSP measures the similarities between neighboring nodes, indicating the smoothing patterns within neighborhoods during propagation. To explore the benefits of NSP, we delve into it in Section 4.1, revealing that NSP exhibits a strong correlation with spectral space and can serve as coefficients for node representations.

A detailed theoretical analysis of ISP and NSP can be found in Section 4.1, which supports the empirical results in Section 1 and motivates our design of SmoothGNN.

4 Method: SmoothGNN

Our observation in Section 1 highlights the different smoothing patterns exhibited by anomalous and normal nodes. In the following sections, we present detailed theoretical analyses and the design of our SmoothGNN. Specifically, Section 4.1 provides a comprehensive theoretical analysis of smoothing patterns, which serves as the motivation behind the design of two key components: SLC and SSGNN, to be elaborated in Sections 4.2 and 4.3, respectively. Moreover, our theoretical analysis in Section 4.1 reveals that the spectral energy of the graph can be represented by NSP, which inspires us to employ it as effective coefficients for node representations, to be detailed in Section 4.4. Finally, Section 4.5 illustrates the overall objective function, including a feature reconstruction loss and the proposed SMeasure.

4.1 Theoretical Analysis of Smoothing Patterns

The smoothing issue has been extensively studied in graph learning. However, previous studies such as [36] primarily focus on its negative aspects. This motivates us to explore the potential positive implications of the smoothing issue. To this end, we conduct a detailed analysis to demonstrate how ISP and NSP can reveal anomalous properties of nodes. All proofs of our theorems can be found in Appendix A.1.

Based on previous research [14, 29], both local views, such as neighboring nodes and their features, and global views, which encompass statistical information of entire graphs, contribute to the detection of node anomalies. The following Theorem 1 indicates that ISP can be represented by an augmented propagation matrix that incorporates both local and global information, suggesting that ISP can be an effective identifier for NAD tasks.

Theorem 1. *Let $\boldsymbol{P} = \frac{\boldsymbol{I_n}+\tilde{\boldsymbol{A}}}{2}$ denote the propagation matrix given the adjacency matrix $\tilde{\boldsymbol{A}}$. For an augmented propagation matrix $\boldsymbol{B}^t = (\boldsymbol{P} - \boldsymbol{P}^\infty)^t$, where $\boldsymbol{P}^\infty$ represents the converged status of $\boldsymbol{P}$, we can derive $\boldsymbol{B}^t = \boldsymbol{P}^t - \boldsymbol{P}^\infty$ with (i, j)-th entry*

$$\boldsymbol{B}_{i,j} = \frac{(2m+n)(\mathbb{I}[i=j]\sqrt{d_i+1} + 2a_{ij}) - 2(d_i+1)\sqrt{d_j+1}}{2\sqrt{d_i+1}(2m+n)},$$

where $\mathbb{I}[\cdot]$ is the indicator function, $a_{i,j}$ is the (i, j)-th entry of the adjacency matrix, d_i is the degree of node i, and m, n represent the number of edges and nodes, respectively.

Theorem 1 shows that when the graph signal $\boldsymbol{x}$ propagates on the augmented propagation matrix $\boldsymbol{B}$, the resulting node representation becomes aware of individual node features and local information, such as edge connections and the degrees of neighbors. Moreover, this matrix not only propagates graph signal through edges but also assigns the signal a transformation of statistical information of graph as coefficients, functioning similarly to an attention mechanism. It highlights the disparities arising from global views. Consequently, the augmented propagation matrix provides a more precise indication of the underlying properties of both anomalous and normal nodes compared to the original matrix. This observation is further supported by the empirical evidence of ISP shown in Section 1. Specifically, the comprehensive information contained in the augmented propagation matrix helps to elucidate the different smoothing processes of anomalous and normal nodes, where anomalous nodes are harder to converge than normal ones. Therefore, we employ this matrix in the design of the Smoothing-aware Learning Component (SLC) in Section 4.2.

In addition to the close relationship between the augmented propagation matrix and graph anomalies established by Theorem 1, previous studies [8, 34] have also shown a strong connection between graph anomalies and the graph spectral space. This motivates us to further investigate the relationships between the augmented propagation matrix and the graph spectral space. The following theorem confirms that column vectors of the augmented propagation matrix can be represented by a polynomial combination of graph convolution operations, indicating a strong correlation between the augmented propagation matrix and the graph spectral space.

Theorem 2. *The augmented propagation matrix $\boldsymbol{B}$ after t hops of propagation can be expressed by $\boldsymbol{b}^t = \sum_{k=0}^{t} \tilde{\boldsymbol{\theta}}_k \boldsymbol{L}^k \boldsymbol{u}\boldsymbol{v}$, where $\boldsymbol{b}^t$ is a column vector of $\boldsymbol{B}^t$, $\tilde{\boldsymbol{\theta}}_k \in \mathbb{R}^n$ is the spectral filter coefficients, and $\boldsymbol{u}, \boldsymbol{v}$ represent the linear combinations of the eigenvectors of $\tilde{\boldsymbol{A}}$ and $\boldsymbol{L}$, respectively.*

Theorem 2 illustrates the connection between the augmented propagation matrix and the graph spectral space. This insight motivates us to design a Smoothing-aware Spectral Graph Neural Network (SSGNN) that not only leverages spectral information but also captures ISP, to be elaborated in Section 4.3. Besides, previous work [34] has shown spectral energy (refer to Definition 1) can serve as an effective identifier for NAD tasks. Given our findings that reveal a strong connection between smoothing patterns and spectral space, we further investigate the relationship between smoothing patterns and spectral energy. First, we provide the definition of spectral energy:

Definition 1 ([8, 34]). *Given the graph Laplacian matrix $\boldsymbol{L} = \boldsymbol{U}\boldsymbol{\Lambda}\boldsymbol{U}^T$ and a graph signal $\boldsymbol{x}$, the graph Fouier Transformation of $\boldsymbol{x}$ is defined as $\hat{\boldsymbol{x}} = \{\hat{x_1}, \cdots, \hat{x_n}\} = \boldsymbol{U}^T\boldsymbol{x}$. The spectral energy of the graph at λ_k can be expressed as $\frac{\hat{x}_k^2}{\sum_{i=1}^n \hat{x}_i^2}$.*

Based on Definition 1, we present the following theorem, which shows that NSP can serve a similar role as spectral energy.

Theorem 3. *Given a graph G with Laplacian matrix $\boldsymbol{L}$ and a graph signal $\boldsymbol{x}$, NSP can be represented by $N(\boldsymbol{x}) = \frac{\boldsymbol{x}^T\boldsymbol{L}\boldsymbol{x}}{\boldsymbol{x}^T\boldsymbol{x}} = \frac{\sum_{j=1}^n \lambda_j \hat{x}_j^2}{\sum_{i=1}^n \hat{x}_i^2}$, where the λ_j is the j-th eigenvalue of $\boldsymbol{L}$.*

Theorem 3 shows that the NSP of nodes can be represented by a polynomial combination of the spectral energy, indicating that NSP can serve as an effective identifier for NAD tasks. Recap from Section 3 that NSP characterizes the smoothing patterns within neighborhoods of nodes, which is complementary to the previous local view depicted by ISP. This motivates us to combine ISP and NSP to derive final representations and establish a novel measure for the anomaly scoring function. Specifically, we introduce Smoothing-aware Coefficients (SC) as the coefficients of node representations to facilitate the identification of different nodes, and Smoothing-aware Measure (SMeasure) as the metric for calculating the anomalous scores, which will be discussed in Sections 4.4 and 4.5, respectively.

So far, we have introduced the intuition behind four key components of SmoothGNN from both empirical and theoretical perspectives. Beyond the design, we further analyze the maximum propagation hops of SmoothGNN that do not provide additional information for NAD tasks. To be specific, if the current node representations have reached a converged state, additional layers of SmoothGNN will not yield substantial benefits but will consume extra computational resources. Therefore, we determine the layers of SmoothGNN based on Theorem 4. To achieve this, we provide ϵ-smoothing [30] and illustrate the theorem of the converged hop.

Definition 2 ([30]). *For any GNN, we call it suffers from ϵ-smoothing if and only if after T hops of propagation, the resulting feature matrix $\boldsymbol{H}^t$ at hop $t \geq T$ has a distance no larger than ϵ with respect to a subspace S, namely, $d_S(\boldsymbol{H}^t) \leq \epsilon, \forall t \geq T$, where $d_S(\boldsymbol{H}^t) := min_{\boldsymbol{M}\in S}||\boldsymbol{H}^t - \boldsymbol{M}||_F$ represents the Frobenius norm from $\boldsymbol{H}^t$ to the subspace S.*

Theorem 4. *Given the subspace S with threshold ϵ, a GNN model will suffer from ϵ-smoothing issue when the propagation hop $t = \left\lceil \frac{\log(\epsilon/d_S(\boldsymbol{X}))}{\log(\tau\lambda)} \right\rceil$, where τ is the largest singular value of the graph filters over all layers, λ is the second largest eigenvalue of the propagation matrix, and $\boldsymbol{X}$ is the feature matrix of graph G.*

Theorem 4 provides a theoretical guarantee regarding the maximum propagation hops that can contribute to the learning process, which provides guidance for choosing the appropriate number of layers in our experiments, as shown in Section 5 and Appendix 5.4. In the following Sections 4.2, 4.3, 4.4, and 4.5, we elaborate on our SmoothGNN framework in detail.

4.2 Smoothing-aware Learning Component

Motivated by Theorem 1, we propose a simple yet powerful component to explicitly capture the ISP of nodes. Specifically, we first calculate the augmented propagation matrix $B^t = P^t - P^\infty$ for $t = 0, \cdots, T$. Next, we employ a set of $(T+1)$ MLPs to obtain the latent node representations propagated on each B^t. Finally, an additional MLP is adopted to fuse the node representations obtained from $(T+1)$ propagation hops. Let $\tilde{X}_t$ denote the node features $\boldsymbol{X}$ after the t-th feature transformation, the representation of the i-th node in SLC can be expressed as:

$$\boldsymbol{h}_i^{SLC} = \text{MLP}(\text{CONCAT}((\boldsymbol{B}^0\tilde{\boldsymbol{X}}_0)_i, \cdots, (\boldsymbol{B}^T\tilde{\boldsymbol{X}}_T)_i)).$$

Despite the simplicity of the SLC module, it can capture the information underlying the ISP of different nodes and thus can serve as an effective component for unsupervised NAD tasks as shown in the later experiments.

In addition to explicitly learning from ISP, capturing information from the graph topology and node features can also be useful to NAD. The combination of explicit and implicit learning enables the collection of comprehensive information required for NAD tasks, which is demonstrated in the ablation study in Section 5.3. The details of implicit learning GNN are presented as follows.

4.3 Smoothing-aware Spectral GNN

As stated in Theorem 2, the column vector of augmented propagation matrix after t hops of propagation can be represented as $\boldsymbol{b}^t = \sum_{t=0}^T \tilde{\boldsymbol{\theta}}_t \boldsymbol{L}^t \boldsymbol{u}\boldsymbol{v}$, demonstrating the capability of the graph spectral space to reveal underlying node properties for NAD. This motivates our design of a spectral GNN to learn node representations. Based on the theoretical analysis, employing a polynomial combination of graph spectral filters as the graph convolution operation can be a natural choice. To maintain the simplicity of our framework, we leverage T-th order polynomial of graph Laplacian as the backbone filter. Specifically, let $g(\boldsymbol{X})_T$ be the graph convolution operation, we have:

$$g(\boldsymbol{X})_T = (\sum_{t=0}^T \theta_t \boldsymbol{L}^t)\boldsymbol{X}.$$

Similar to SLC, we consider $\tilde{\boldsymbol{X}}_t$ as node features after t-th feature transformation for each graph convolution operation. Subsequently, we employ an MLP to fuse the spectral node representations obtained from each propagation hop to generate final node representations. The representation of i-th node can be expressed as:

$$\boldsymbol{h}_i^{GNN} = \text{MLP}(\text{CONCAT}((g(\tilde{\boldsymbol{X}}_0)_0)_i, \cdots, (g(\tilde{\boldsymbol{X}}_T)_T)_i)).$$

Note that we utilize shared weights in SLC and SSGNN, so that the learnable weights can be influenced by both components simultaneously, which makes the assistance of feature reconstruction for SMeasure in Section 4.5 more effective. By incorporating these two components, our framework can capture information from both spectral space and smoothing patterns.

In addition, as discussed in Section 4.1, combining ISP and NSP will enable the framework to effectively distinguish anomalous nodes and normal nodes. Hence, we utilize NSP as the coefficients for SLC and SSGNN components to achieve this goal. The details of SC will be further introduced in Section 4.4.

4.4 Smoothing-aware Coefficients

Theorem 3 shows that NSP can be interpreted as a polynomial combination of spectral energy, which is an effective identifier of NAD tasks as shown in previous works [8, 34]. Motivated by the results, we design SC as coefficients for node representations. Specifically, we calculate the linear combination of $(T+1)$ hops of NSP based on Theorem 3, which can be expressed as:

$$SC(\boldsymbol{X}) = diag\left(\frac{\boldsymbol{X}^T\boldsymbol{L}\boldsymbol{X}}{\boldsymbol{X}^T\boldsymbol{X}}\right),$$
$$\boldsymbol{\alpha} = \sigma(\text{MLP}(\text{CONCAT}(SC(\boldsymbol{P}^0\tilde{\boldsymbol{X}}_0), \cdots, SC(\boldsymbol{P}^T\tilde{\boldsymbol{X}}_T)))),$$

where $diag(\cdot)$ denotes the diagonal entries of a square matrix, and $\sigma(\cdot)$ is the Sigmoid function. Then, we utilize element-wise multiplication $*$ to modify representations $\boldsymbol{h}_i^{SLC}$ and $\boldsymbol{h}_i^{GNN}$:

$$\boldsymbol{h}_i^{SCSLC} = \boldsymbol{h}_i^{SLC} * \boldsymbol{\alpha}, \boldsymbol{h}_i^{SCGNN} = \boldsymbol{h}_i^{GNN} * \boldsymbol{\alpha}.$$

The final representations generated by SLC and SSGNN with the assistance of SC are utilized to calculate the loss function and SMeasure, which will be illustrated in the following section.

4.5 Smoothing-aware Measure

According to previous work [17], feature reconstruction loss can assist in learning effective measures for NAD. This inspires us to design a loss function combined with two components: the feature reconstruction loss and SMeasure. For the feature reconstruction loss, we use $\boldsymbol{h}_i^{SCGNN}$ to reconstruct the original feature:

$$L_{con} = \frac{1}{n}\sum_{i=1}^n ||\boldsymbol{h}_i^{SCGNN} - \boldsymbol{x}_i||_2,$$

where $\boldsymbol{x}_i$ is the i-th row of the original feature matrix $\boldsymbol{X}$. For SMeasure, we leverage the representations obtained from SLC as it naturally captures the underlying properties in the smoothing patterns.

To be specific, we define SMeasure as follows:

$$f_{smooth}(\boldsymbol{h}_i^{SCSLC}) = \sigma(\text{AVG}(\boldsymbol{h}_i^{SCSLC})),$$

where $\sigma(\cdot)$ represents the Sigmoid function, and AVG$(\cdot)$ represents the column-wise average function. Based on SMeasure, we further define the smoothing-aware loss function:

$$L_{smooth} = \frac{1}{n}\sum_{i=1}^{n} f_{smooth}(\boldsymbol{h}_i^{SCSLC}).$$

The final loss function is a combination of both L_{con} and L_{smooth}:

$$L = L_{con} + L_{smooth}.$$

The loss function is carefully designed to leverage the feature reconstruction loss to facilitate the learning process of SMeasure. This combination enables the loss function to capture valuable information from the smoothing patterns and the reconstruction errors across different nodes, which can be demonstrated in Section 5.3. Minimizing this loss function empowers the model to effectively reduce the ratio of anomalous nodes in the predicted results, thereby addressing the challenge of extremely unbalanced data in NAD. With this comprehensive loss function, our SmoothGNN can optimize the shared weights of two key components. Consequently, our framework excels in learning more accurate node representations for the task of detecting anomalous nodes.

5 Experiments

5.1 Experimental Setup

Datasets. We evaluate SmoothGNN on 9 real-world datasets, including Reddit, Tolokers, Amazon, T-Finance, YelpChi, Questions, Elliptic, DGraph-Fin, and T-Social. These datasets are obtained from the benchmark paper [33], consisting of various types of networks and corresponding anomalous nodes. Based on their number of nodes, we divide these datasets into three categories, Small, Medium, and Large, as shown in Appendix A.4. Note that, unlike previous works in the unsupervised NAD area, we only utilize real-world datasets with a sufficient number of nodes. To the best of our knowledge, SmoothGNN is the only model in this field that conducts comprehensive experiments on large-scale datasets such as T-Social to validate the efficiency and effectiveness of various models.

Baselines. We compare SmoothGNN against 11 state-of-the-art competitors, including shallow models, reconstruction models, self-supervised models, and special models.

- Shallow models: RADAR [21], and ANOMALOUS [28].
- Reconstruction models: CLAD [18] and GADNR [31].
- Self-supervised models: NLGAD [13], GRADATE [11], PREM [27], ARISE [12], and TAM [29].
- Special models: RAND [4], VGOD [17], and REC [15].

Experimental Settings. In line with the experimental settings of prior studies, such as [17, 22, 29], we conduct transductive experiments on these datasets. The parameters of SmoothGNN are set according to the categories of the datasets. The specific parameters for each category can be found in Appendix A.4. To ensure a fair comparison, we obtain the source code of all competitors from GitHub and execute these models using the default parameter settings suggested by their authors.

Comparison Metrics. To provide fair comparison results, we follow previous works in this area, utilizing AUC and Average Precision (AP) as the metrics for comparison. Specifically, AUC provides an aggregate measure of performance across all possible classification thresholds. One way of interpreting AUC is the probability that the model ranks a random positive example more highly than a random negative example. AP provides insights into the precision of anomaly detection at all decision thresholds. It calculates the area under the Precision-Recall curve, which balances the effects of precision and recall. A higher AP indicates a lower false-positive rate and false-negative rate. As a result, if a framework can achieve higher AUC and AP than other frameworks, it is comprehensive enough to show that such a framework is effective for unsupervised NAD tasks. Moreover, we also report the running time cost to demonstrate the efficiency of our framework.

5.2 Main Results

We evaluate the performance of SmoothGNN against different state-of-the-art competitors in the field of unsupervised NAD. Table 1 reports the AUC and AP scores of each model across 9 datasets and Table 2 reports their running times. The best result on each dataset is highlighted in boldface. Our key observations are as follows.

Firstly, most existing unsupervised NAD models struggle to handle large datasets, with only VGOD, REC, and the proposed SmoothGNN successfully running on the two largest datasets. This highlights the need for the development of unsupervised models capable of handling large-scale datasets.

Shallow models, Radar and ANOMALOUS, apply residual analysis to solve NAD, which poses challenges in capturing the underlying anomalous properties from a spectral perspective. In comparison, SmoothGNN takes the lead by 29.37% and 29.03% in terms of AUC, and 11.52% and 11.63% in terms of AP on average across 6 datasets, respectively. Moreover, these shallow models are unable to handle the 3 large datasets due to memory constraints. These results demonstrate that shallow models are both time-consuming and ineffective when applied to real-world NAD datasets.

Next, we examine reconstruction models, CLAD and GADNR, which utilize reconstruction techniques to detect graph anomalies. While these models leverage both structure and feature reconstruction to calculate the anomalous score for each node, they fail to utilize a more effective identifier, such as smoothing patterns, leading to inferior performance. SmoothGNN outperforms these models by 26.14% and 17.75% in terms of AUC, and 10.31% and 8.30% in terms of AP on average across different datasets, respectively.

We then compare SmoothGNN with self-supervised models, NLGAD, GRADATE, PREM, ARISE, and TAM. Although self-supervised models can boost the performance of unsupervised frameworks, their high memory requirements and computational costs make them prohibitive for large datasets. While NLGAD and PREM utilize sparse techniques to address these issues, they still cannot run on the two largest datasets. In comparison, SmoothGNN achieves an improvement of 14.95% and 17.66% in terms of AUC, and 8.44% and 8.63% in terms of AP on average across 7 datasets, respectively. Besides, SmoothGNN also outperforms GRADATE and ARISE by 18.41% and 16.12% in terms of AUC, and 10.28% and 9.53% in terms of AP on average across 7 datasets, respectively. In addition, TAM

Table 1: AUC and Precision (%) on 9 datasets, where "-" represents failed experiments due to memory constraint. The best result on each dataset is highlighted in boldface.

		Shallow		Reconstruction		Self-supervised					Special			
Datasets	Metrics	RADAR	ANOMALOUS	CLAD	GADNR	NLGAD	GRADATE	PREM	ARISE	TAM	RAND	VGOD	REC	SmoothGNN
Reddit	AUC	0.4372	0.4481	0.5784	0.5532	0.5380	0.5261	0.5518	0.5273	0.5729	0.5417	0.4931	0.5510	**0.5946**
	AP	0.0273	0.0309	**0.0502**	0.0373	0.0415	0.0393	0.0413	0.0402	0.0425	0.0356	0.0324	0.0421	0.0438
Tolokers	AUC	0.3625	0.3706	0.4061	0.5768	0.4825	0.5373	0.5654	0.5514	0.4699	0.4377	0.4988	0.4314	**0.6870**
	AP	0.1713	0.1731	0.1921	0.2991	0.2025	0.2364	0.2590	0.2505	0.1963	0.1939	0.2212	0.1946	**0.3517**
Amazon	AUC	0.2318	0.2318	0.2026	0.2608	0.5425	0.4781	0.2782	0.4782	0.8028	0.3585	0.5182	0.5869	**0.8408**
	AP	0.0439	0.0439	0.0401	0.0424	0.0991	0.0634	0.0744	0.0677	0.3322	0.0492	0.0779	0.1349	**0.3953**
T-Finance	AUC	0.2824	0.2824	0.1385	0.5798	0.5231	0.4063	0.4484	0.4667	0.6901	0.4380	0.4814	0.5239	**0.7556**
	AP	0.0295	0.0295	0.0247	0.0542	0.0726	0.0376	0.0391	0.0393	0.1284	0.0403	0.0454	0.0454	**0.1408**
YelpChi	AUC	0.5261	0.5272	0.4755	0.4704	0.4981	0.4920	0.4900	0.4834	0.5487	0.5052	0.4878	0.5134	**0.5758**
	AP	0.1822	0.1700	0.1284	0.1395	0.1469	0.1447	0.1378	0.1415	0.1733	0.1470	0.1345	0.1623	**0.1823**
Questions	AUC	0.4963	0.4965	0.6207	0.5875	0.5428	0.5539	0.6033	0.6241	0.5042	0.6164	0.5075	0.4988	**0.6444**
	AP	0.0279	0.0279	0.0512	0.0577	0.0348	0.0350	0.0430	**0.0619**	0.0395	0.0442	0.0299	0.0279	0.0592
Elliptic	AUC	-	-	0.4192	0.4001	0.4977	-	0.4978	-	-	-	0.5723	**0.5848**	0.5729
	AP	-	-	0.0807	0.0778	0.1009	-	0.0905	-	-	-	0.1256	**0.1337**	0.1161
DGraph-Fin	AUC	-	-	-	-	-	-	-	-	-	-	0.5456	0.4710	**0.6499**
	AP	-	-	-	-	-	-	-	-	-	-	0.0148	0.0112	**0.0199**
T-Social	AUC	-	-	-	-	-	-	-	-	-	-	0.5999	0.0793	**0.7034**
	AP	-	-	-	-	-	-	-	-	-	-	0.0351	0.0157	**0.0631**

Table 2: Running time (s) on 9 datasets, where "-" represents failed experiments due to memory constraint. The best result on each dataset is highlighted in boldface.

	Shallow		Reconstruction		Self-supervised					Special			
Datasets	RADAR	ANOMALOUS	CLAD	GADNR	NLGAD	GRADATE	PREM	ARISE	TAM	RAND	VGOD	REC	SmoothGNN
Reddit	55.57	42.25	11.14	692.66	10886.19	7562.59	73.52	1261.99	5050.89	310.11	39.86	83.23	**7.02**
Tolokers	57.51	40.94	52.91	861.95	10504.91	7824.63	74.80	1281.71	5668.91	367.03	177.42	161.54	**6.99**
Amazon	42.79	38.07	431.20	2048.72	10649.83	7856.41	130.57	1267.38	1148.24	593.75	1517.70	2558.55	**7.19**
T-Finance	500.19	360.97	2161.16	14255.00	35648.72	30341.65	266.33	4223.50	81238.60	6746.10	5998.08	83339.64	**16.69**
YelpChi	730.81	513.83	418.95	5046.51	42435.07	35938.21	308.68	5042.99	102232.07	6588.60	1283.10	978.22	**19.37**
Questions	1205.05	1114.22	52.65	2795.99	51270.03	44235.87	409.45	6135.88	11603.81	7364.07	86.12	482.32	**32.68**
Elliptic	-	-	421.17	12568.50	193304.73	-	2149.77	-	-	-	231.63	566.79	**205.10**
DGraph-Fin	-	-	-	-	-	-	-	-	-	-	3420.84	6795.90	**2924.99**
T-Social	-	-	-	-	-	-	-	-	-	-	22984.10	80388.98	**4877.05**

is the best rival in terms of performance, but its high memory usage and running time make it unable to run on large datasets. Across 6 datasets, SmoothGNN surpasses TAM by 8.49% in terms of AUC and 4.35% in terms of AP on average. Finally, we examine the results of special models, RAND, VGOD and REC. RAND represents a novel direction for unsupervised NAD tasks but fails to leverage more advanced properties, such as smoothing patterns, to guide the learning process. As a result, SmoothGNN outperforms RAND by 20.01% in terms of AUC, and 11.05% in terms of AP on average across 6 datasets. On the other hand, VGOD and REC are the only two competitors capable of running on all the datasets, demonstrating the benefits of designing efficient measures for unsupervised NAD tasks. For instance, REC utilizes a dissimilarity measure integrating Dirichlet Energy to calculate the anomalous score for each node, enhancing REC's ability to capture information from smoothing patterns within the neighborhood. However, SmoothGNN leverages a novel measure more efficiently and effectively, surpassing VGOD and REC by 14.66% and 19.82% in terms of AUC, and 7.28% and 6.72% in terms of AP on average across all datasets, respectively. Moreover, with VGOD as the most efficient and effective competitor, our SmoothGNN outperforms it in all datasets with a 75x speed-up in running time, which demonstrates the usefulness of our framework.

5.3 Ablation Study

The ablation study for SC is presented in Table 3. Notably, without SC to rearrange the weights of different dimensions in the spectral space, the performance drops significantly compared to the original SmoothGNN, which demonstrates the utilization of SC can boost the performances. It also underscores that capturing the smoothing patterns from different views will help the learning of the node representations for NAD tasks. Moreover, without the assistance of feature reconstruction in the loss function, the performance of SmoothGNN will also drop to some extent as shown in Table 3, which proves the benefits of feature reconstruction as the assistance for the learning process. This phenomenon matches the results in previous works such as [17], highlighting the rationality of utilizing feature reconstruction in our framework.

Table 3: Ablation study.

Datasets	Reddit		Tolokers		Amazon		T-Finance		YelpChi		Questions		Elliptic		DGraph-Fin		T-Social	
Metrics	AUC	AP	AUC	AP	AUC	AP	AUC	AP	AUC	AP	AUC	AP	AUC	AP	AUC	AP	AUC	AP
SmoothGNN	0.5946	0.0438	0.6870	0.3517	0.8408	0.3953	0.7556	0.1408	0.5758	0.1823	0.6444	0.0592	0.5729	0.1161	0.6499	0.0199	0.7034	0.0631
w/o SC	0.5437	0.0356	0.6115	0.2967	0.5131	0.0645	0.2869	0.0292	0.5715	0.1770	0.6260	0.0630	0.5596	0.1076	0.5868	0.0161	0.6639	0.0622
w/o L_{con}	0.5801	0.0494	0.6645	0.3168	0.8106	0.3031	0.7311	0.0858	0.5608	0.1719	0.6335	0.0506	0.5655	0.1145	0.6189	0.0181	0.6715	0.0514

Table 4: AUC and Precision (%) on 8 datasets of SmoothGNN and SmoothGNN-A. Due to the high computational cost of SmoothGNN-A, we omit the results on the largest T-Social dataset.

Datasets	Reddit		Tolokers		Amazon		T-Finance		YelpChi		Questions		Elliptic		DGraph-Fin	
Metrics	AUC	AP	AUC	AP	AUC	AP	AUC	AP	AUC	AP	AUC	AP	AUC	AP	AUC	AP
SmoothGNN	0.5946	0.0438	0.6870	0.3517	0.8408	0.3953	0.7556	0.1408	0.5758	0.1823	0.6444	0.0592	0.5729	0.1161	0.6499	0.0199
SmoothGNN-A	0.5919	0.0486	0.6731	0.3340	0.8008	0.2719	0.7408	0.1099	0.5697	0.1887	0.6388	0.0527	0.5695	0.1136	0.5893	0.0164

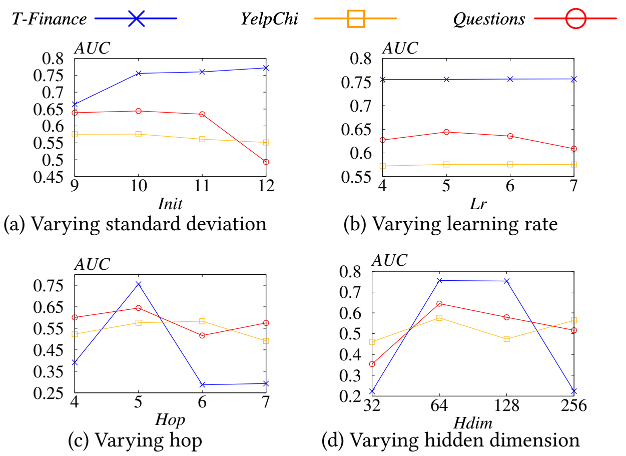

(a) Varying standard deviation (b) Varying learning rate

(c) Varying hop (d) Varying hidden dimension

Figure 3: Varying the standard deviation, learning rate, hop, and hidden dimension.

5.4 Parameter Analysis

Next, we conduct experiments to analyze the effect of representative parameters: the standard deviation of weight initialization, the learning rate, the number of propagation hops, and the hidden dimension of SmoothGNN on T-Finance, YelpChi, and Questions datasets. Figure 3 reports the AUC of SmoothGNN as we vary the standard deviation from 9e-3 to 12e-3, the learning rate from 4e-4 to 7e-4, the hop from 4 to 7, and the hidden dimension from 32 to 256. As we can observe, when we set the standard deviation to 10e-3, SmoothGNN achieves relatively satisfactory performances across these three datasets. In terms of learning rate, SmoothGNN exhibits relatively stable performance, but we can identify an optimal one, so we set the learning rate to 5e-5. Meanwhile, SmoothGNN shows a relatively stable and high performance in terms of all three presented datasets when we set the hop to 5. As a result, the hop is set to 5 in SmoothGNN. Besides, when setting the hidden dimension to 64, our SmoothGNN achieves the best performance. Hence, the hidden dimension in experiments are set to 64.

5.5 Alternative Smoothing Patterns

In addition to the smoothing patterns observed in vanilla GNN, other graph learning models with different propagation methods, such as [10, 35, 37, 38], can show similar properties. For instance, APPNP [20] is one of the most common design within the area of PPR-based Graph Neural Networks, which can also converge to a steady state. The converged state of APPNP is expressed as:

$$\boldsymbol{Z}^{\infty} = \alpha(\boldsymbol{I}_n - (1-\alpha)\boldsymbol{A})^{-1}\boldsymbol{X},$$

where α is the teleport probability. To investigate whether any smoothing pattern can be utilized for detecting anomalous nodes, we modify the graph convolution operation in SSGNN with APPNP update rule $\boldsymbol{Z}^t = (1-\alpha)\boldsymbol{A}\boldsymbol{Z}^{t-1} + \alpha\boldsymbol{X}$, and replace $\boldsymbol{B}^t$ with $\boldsymbol{Z}^t - \boldsymbol{Z}^{\infty}$. The results of this modified model, denoted as SmoothGNN-A, are shown in Table 4. Due to the high computational complexity of the inversion of a matrix, we only report 8 datasets for SmoothGNN-A. We observe that by employing alternative smoothing patterns, the framework can still effectively detect anomalous nodes, thus validating that smoothing patterns serve as accurate identifiers for NAD. However, based on the comparison between SmoothGNN and SmoothGNN-A in Table 4, we find SmoothGNN can achieve relatively better performance in most datasets. These results demonstrate information from spectral space is also important in NAD.

6 Conclusion

In this paper, we introduce the individual and neighborhood smoothing patterns into the NAD task. We identify differences in the smoothing patterns between anomalous and normal nodes and further demonstrate the observation through comprehensive experiments and theoretical analysis. The combination of four components in SmoothGNN enables the model to capture information from both the spectral space and smoothing patterns, providing comprehensive perspectives for NAD tasks. Extensive experiments demonstrate that SmoothGNN consistently outperforms state-of-the-art competitors by a significant margin in terms of performance and running time, thus highlighting the effectiveness and efficiency of leveraging smoothing patterns in the NAD area.

Acknowledgments

This work is supported by the RGC GRF grant (No. 14217322), Hong Kong ITC ITF grant (No. MRP/071/20X), and Tencent Rhino-Bird Focused Research Grant.

References

[1] Leman Akoglu, Hanghang Tong, and Danai Koutra. 2015. Graph based anomaly detection and description: a survey. *Data Min. Knowl. Discov.* 29, 3 (2015), 626–688.

[2] Sambaran Bandyopadhyay, Lokesh N, Saley Vishal Vivek, and M. Narasimha Murty. 2020. Outlier Resistant Unsupervised Deep Architectures for Attributed Network Embedding. In *WSDM*. 25–33.

[3] Sambaran Bandyopadhyay, Lokesh Nagalapatti, and M. Narasimha Murty. 2019. Outlier Aware Network Embedding for Attributed Networks. In *AAAI*. 12–19.

[4] Yuanchen Bei, Sheng Zhou, Qiaoyu Tan, Hao Xu, Hao Chen, Zhao Li, and Jiajun Bu. 2023. Reinforcement Neighborhood Selection for Unsupervised Graph Anomaly Detection. In *ICDM*. 11–20.

[5] Ming Chen, Zhewei Wei, Zengfeng Huang, Bolin Ding, and Yaliang Li. 2020. Simple and Deep Graph Convolutional Networks. In *ICML*. 1725–1735.

[6] F. R. K. Chung. 1997. *Spectral Graph Theory*. American Mathematical Society.

[7] Michaël Defferrard, Xavier Bresson, and Pierre Vandergheynst. 2016. Convolutional Neural Networks on Graphs with Fast Localized Spectral Filtering. In *NeurIPS*. 3837–3845.

[8] Xiangyu Dong, Xingyi Zhang, and Sibo Wang. 2024. Rayleigh Quotient Graph Neural Networks for Graph-level Anomaly Detection. In *ICLR*.

[9] Yingtong Dou, Zhiwei Liu, Li Sun, Yutong Deng, Hao Peng, and Philip S. Yu. 2020. Enhancing Graph Neural Network-based Fraud Detectors against Camouflaged Fraudsters. In *CIKM*. 315–324.

[10] Xinyu Du, Xingyi Zhang, Sibo Wang, and Zengfeng Huang. 2023. Efficient Tree-SVD for Subset Node Embedding over Large Dynamic Graphs. *Proc. ACM Manag. Data* 1, 1 (2023), 96:1–96:26.

[11] Jingcan Duan, Siwei Wang, Pei Zhang, En Zhu, Jingtao Hu, Hu Jin, Yue Liu, and Zhibin Dong. 2023. Graph Anomaly Detection via Multi-Scale Contrastive Learning Networks with Augmented View. In *AAAI*. 7459–7467.

[12] Jingcan Duan, Bin Xiao, Siwei Wang, Haifang Zhou , and Xinwang Liu. 2023. Arise: Graph anomaly detection on attributed networks via substructure awareness. *TNNLS* 35, 12 (2023), 1–14.

[13] Jingcan Duan, Pei Zhang, Siwei Wang, Jingtao Hu, Hu Jin, Jiaxin Zhang, Haifang Zhou, and Xinwang Liu. 2023. Normality Learning-based Graph Anomaly Detection via Multi-Scale Contrastive Learning. In *MM*. 7502–7511.

[14] Yuan Gao, Xiang Wang, Xiangnan He, Zhenguang Liu, Huamin Feng, and Yongdong Zhang. 2023. Addressing Heterophily in Graph Anomaly Detection: A Perspective of Graph Spectrum. In *WWW*. 1528–1538.

[15] Dmitrii Gavrilev and Evgeny Burnaev. 2023. Anomaly Detection in Networks via Score-Based Generative Models. In *ICML Workshop SPIGM*. 1–16.

[16] Xuanwen Huang, Yang Yang, Yang Wang, Chunping Wang, Zhisheng Zhang, Jiarong Xu, Lei Chen, and Michalis Vazirgiannis. 2022. DGraph: A Large-Scale Financial Dataset for Graph Anomaly Detection. In *NeurIPS*. 22765–22777.

[17] Yihong Huang, Liping Wang, Fan Zhang, and Xuemin Lin. 2023. Unsupervised Graph Outlier Detection: Problem Revisit, New Insight, and Superior Method. In *ICDE*. 2565–2578.

[18] Junghoon Kim, Yeonjun In, Kanghoon Yoon, Junmo Lee, and Chanyoung Park. 2023. Class Label-aware Graph Anomaly Detection. In *CIKM*. 4008–4012.

[19] Thomas N. Kipf and Max Welling. 2017. Semi-Supervised Classification with Graph Convolutional Networks. In *ICLR*.

[20] Johannes Klicpera, Aleksandar Bojchevski, and Stephan Günnemann. 2019. Predict then Propagate: Graph Neural Networks meet Personalized PageRank. In *ICLR*.

[21] Jundong Li, Harsh Dani, Xia Hu, and Huan Liu. 2017. Radar: Residual Analysis for Anomaly Detection in Attributed Networks. In *IJCAI*. 2152–2158.

[22] Kay Liu, Yingtong Dou, Yue Zhao, Xueying Ding, Xiyang Hu, Ruitong Zhang, Kaize Ding, Canyu Chen, Hao Peng, Kai Shu, Lichao Sun, Jundong Li, George H. Chen, Zhihao Jia, and Philip S. Yu. 2022. BOND: Benchmarking Unsupervised Outlier Node Detection on Static Attributed Graphs. In *NeurIPS*. 27021–27035.

[23] Yang Liu, Xiang Ao, Zidi Qin, Jianfeng Chi, Jinghua Feng, Hao Yang, and Qing He. 2021. Pick and Choose: A GNN-based Imbalanced Learning Approach for Fraud Detection. In *WWW*. 3168–3177.

[24] Xiaoxiao Ma, Jia Wu, Shan Xue, Jian Yang, Chuan Zhou, Quan Z. Sheng, Hui Xiong, and Leman Akoglu. 2023. A Comprehensive Survey on Graph Anomaly Detection With Deep Learning. *IEEE Trans. Knowl. Data Eng.* 35, 12 (2023), 12012–12038.

[25] Julian J. McAuley and Jure Leskovec. 2013. From amateurs to connoisseurs: modeling the evolution of user expertise through online reviews. In *WWW*. 897–908.

[26] Kenta Oono and Taiji Suzuki. 2019. On Asymptotic Behaviors of Graph CNNs from Dynamical Systems Perspective. *ArXiv* abs/1905.10947 (2019).

[27] Junjun Pan, Yixin Liu, Yizhen Zheng, and Shirui Pan. 2023. PREM: A Simple Yet Effective Approach for Node-Level Graph Anomaly Detection. In *ICDM*. 1253–1258.

[28] Zhen Peng, Minnan Luo, Jundong Li, Huan Liu, and Qinghua Zheng. 2018. ANOMALOUS: A Joint Modeling Approach for Anomaly Detection on Attributed Networks. In *IJCAI*. 3513–3519.

[29] Hezhe Qiao and Guansong Pang. 2023. Truncated Affinity Maximization: One-class Homophily Modeling for Graph Anomaly Detection. In *NeurIPS*. 49490–49512.

[30] Yu Rong, Wenbing Huang, Tingyang Xu, and Junzhou Huang. 2020. DropEdge: Towards Deep Graph Convolutional Networks on Node Classification. In *ICLR*.

[31] Amit Roy, Juan Shu, Jia Li, Carl Yang, Olivier Elshocht, Jeroen Smeets, and Pan Li. 2024. GAD-NR: Graph Anomaly Detection via Neighborhood Reconstruction. In *WSDM*. 576–585.

[32] Shuyuan Sun, Yiyang Jiang, Fan Yang, Bei Yu, and Xuan Zeng. 2022. Efficient Hotspot Detection via Graph Neural Network. In *DATE*. 1233–1238.

[33] Jianheng Tang, Fengrui Hua, Ziqi Gao, Peilin Zhao, and Jia Li. 2023. GADBench: Revisiting and Benchmarking Supervised Graph Anomaly Detection. In *NeurIPS*. 29628–29653.

[34] Jianheng Tang, Jiajin Li, Ziqi Gao, and Jia Li. 2022. Rethinking Graph Neural Networks for Anomaly Detection. In *ICML*. 21076–21089.

[35] Kun Xie, Xiangyu Dong, Yusong Zhang, Xingyi Zhang, Qintian Guo, and Sibo Wang. 2024. Learning-Based Attribute-Augmented Proximity Matrix Factorization for Attributed Network Embedding. *TKDE* 36, 11 (2024), 6517–6531.

[36] Wentao Zhang, Mingyu Yang, Zeang Sheng, Yang Li, Wen Ouyang, Yangyu Tao, Zhi Yang, and Bin Cui. 2021. Node Dependent Local Smoothing for Scalable Graph Learning. In *NeurIPS*. 20321–20332.

[37] Xingyi Zhang, Zixuan Weng, and Sibo Wang. 2024. Towards Deeper Understanding of PPR-based Embedding Approaches: A Topological Perspective. In *WWW*. 969–979.

[38] Xingyi Zhang, Kun Xie, Sibo Wang, and Zengfeng Huang. 2021. Learning Based Proximity Matrix Factorization for Node Embedding. In *KDD*. 2243–2253.

[39] Kaixiong Zhou, Xiao Huang, Daochen Zha, Rui Chen, Li Li, Soo-Hyun Choi, and Xia Hu. 2021. Dirichlet Energy Constrained Learning for Deep Graph Neural Networks. In *NeurIPS*. 21834–21846.

A Appendix

A.1 Proofs

Proof of Theorem 1. The following result is used for the proof.

LEMMA 1 ([5]). *Let $\boldsymbol{P} = \frac{\boldsymbol{I_n}}{2} + \frac{\tilde{\boldsymbol{A}}}{2}$ denote the propagation matrix given the adjacency matrix $\tilde{\boldsymbol{A}}$, we have:*

$$\boldsymbol{P}^{\infty}_{i,j} = \frac{\sqrt{d_i+1}\sqrt{d_j+1}}{2m+n}.$$

First, we derive $\boldsymbol{P}^t - \boldsymbol{P}^{\infty} = (\boldsymbol{P} - \boldsymbol{P}^{\infty})^t$. For $t \geq 1$, we have:

$$\begin{aligned}(\boldsymbol{P} - \boldsymbol{P}^{\infty})^t &= \sum_{k=0}^{t}\binom{t}{k}(-1)^k \boldsymbol{P}^{t-k}\boldsymbol{P}^{\infty} = \boldsymbol{P}^t + \sum_{k=1}^{t}\binom{t}{k}(-1)^k \boldsymbol{P}^{\infty} \\ &= \boldsymbol{P}^t + \boldsymbol{P}^{\infty}((1-1)^n - 1) = \boldsymbol{P}^t - \boldsymbol{P}^{\infty}.\end{aligned}$$

Then, we can derive that

$$\begin{aligned}\boldsymbol{B}_{i,j} &= \boldsymbol{P}_{i,j} - \boldsymbol{P}^{\infty}_{i,j} \\ &= \frac{(2m+n)(\mathbb{I}[i=j]\sqrt{d_i+1} + 2a_{ij}) - 2(d_i+1)\sqrt{d_j+1}}{2\sqrt{d_i+1}(2m+n)}.\end{aligned}$$

Then Theorem 1 can be proved. □

Proof of Theorem 2. With proofs in Sec. "The stable distribution" in [6], for column vector $\boldsymbol{b}^t$ in augmented matrix $\boldsymbol{B}^t$, we have:

$$\boldsymbol{b}^t = \boldsymbol{D}^{\frac{1}{2}} \sum_{i=2}^{n} \omega_i^t c_i \boldsymbol{\psi}_i,$$

where $\boldsymbol{D}$ is the degree matrix of graph G, ω_i is the i-th eigenvalue of $\boldsymbol{P}$, $\boldsymbol{\psi}_i$ is the i-th eigenvector of $\tilde{\boldsymbol{A}}$, and c_i is the coefficient related to $\boldsymbol{\psi}_i$. Then, let λ_i^L be the i-th eigenvalue of $\boldsymbol{L}$ and λ_i^A be the i-th eigenvalue of $\tilde{\boldsymbol{A}}$, we have:

$$\lambda_i^L = 1 - \lambda_i^A = 1 - (2\omega_i - 1) = 2 - 2\omega_i.$$

Then we replace ω_i in $\boldsymbol{D}^{\frac{1}{2}} \sum_{i=2}^{n} \omega_i^t c_i \boldsymbol{\psi}_i$ with λ_i^L, we further have $\boldsymbol{D}^{\frac{1}{2}} \sum_{i=2}^{n} (\frac{\lambda_i^L}{2} - 1)^t c_i \boldsymbol{\psi}_i$. Applying Tayler's expansion to it, we have:

$$\begin{aligned}\sum_{i=2}^{n} (\frac{\lambda_i^L}{2} - 1)^t &= \sum_{i=2}^{n} \sum_{k=0}^{t} \frac{t!}{(k-1)!(t-(k-1))!} (\frac{\lambda_i^L}{2})^{k-1} (-1)^{t-(k-1)} \\ &= \sum_{k=0}^{t} \sum_{i=2}^{n} \frac{t!}{(k-1)!(t-(k-1))!} (\frac{\lambda_i^L}{2})^{k-1} (-1)^{t-(k-1)} \\ &= \sum_{k=0}^{t} \frac{(\frac{1}{2})^{k-1} (-1)^{t-(k-1)} t!}{(k-1)!(t-(k-1))!} \sum_{i=2}^{n} (\lambda_i^L)^{k-1} \\ &= \sum_{k=0}^{t} \theta_k \boldsymbol{\Lambda}^k \mathbf{1} = \sum_{k=0}^{t} \theta_k \boldsymbol{U}^T \boldsymbol{U} \boldsymbol{\Lambda}^k \boldsymbol{U}^T \boldsymbol{U} \mathbf{1} = \sum_{k=0}^{t} \tilde{\theta}_k \boldsymbol{L}^k \boldsymbol{u}.\end{aligned}$$

Finally, we can get

$$\boldsymbol{b}^t = \boldsymbol{D}^{\frac{1}{2}} \sum_{i=2}^{n} (\frac{\lambda_i^L}{2} - 1)^t c_i \boldsymbol{\psi}_i = \sum_{k=0}^{t} \tilde{\theta}_k \boldsymbol{L}^k \boldsymbol{u} \boldsymbol{v}.$$

This finishes the proof of Theorem 2. □

Proof of Theorem 3. For simplicity, let $\boldsymbol{x}$ denote a normalized graph signal in the graph, we have:

$$N(\boldsymbol{x}) = \sum_{i,j=1}^{n} a_{i,j} \| \frac{x_i}{\sqrt{d_i + 1}} - \frac{x_j}{\sqrt{d_j + 1}} \|_2^2 = \boldsymbol{x} \boldsymbol{L} \boldsymbol{x}.$$

Following the theorem in previous work [8], we have:

$$\sum_{j=1}^{n} \lambda_j \hat{x}_j^2 = \boldsymbol{x}^T \boldsymbol{L} \boldsymbol{x}.$$

Then Theorem 3 can be proved. □

Proof of Theorem 4. We use the result below for the proof.

Corollary 1 ([26]). *Let $\lambda_1 \leq \cdots \leq \lambda_n$ be the eigenvalues of $\boldsymbol{P}$. Suppose the multiplicity of the largest eigenvalue λ_n is $m (\leq n)$, i.e.,$\lambda_{n-m} < \lambda_{n-m+1} = \cdots = \lambda_n$. The second largest eigenvalue can be defined as*

$$\lambda := max_{s=1}^{n-m} |\lambda_s| < |\lambda_n|.$$

Let U be the eigenspace associated with λ_n, where U has an orthonormal basis that consists of non-negative vectors, and then we have:

$$d_S(\boldsymbol{H}^t) \leq \tau_t \lambda d_S(\boldsymbol{H}^{t-1}),$$

where $\tau_t \lambda < 1$ implies the output of the t-th layer of GNN on G exponentially approaches S.

Based on the above corollary, we have:

$$d_S(\boldsymbol{H}^t) \leq \tau_t \lambda d_S(\boldsymbol{H}^{t-1}) \leq (\prod_{i=1}^{t} \tau_i) \lambda^t d_S(\boldsymbol{X}) \leq \tau^t \lambda^t d_S(\boldsymbol{X}).$$

When the GNN reaches ϵ-smoothing, we have:

$$d_S(\boldsymbol{H}^t) \leq \tau^t \lambda^t d_S(\boldsymbol{X}) \leq \epsilon \rightarrow t \log \tau\lambda < \log\left(\epsilon / d_S(\boldsymbol{X})\right).$$

Since $0 \leq s\lambda < 1$, then we have $\log s\lambda < 0$, we have:

$$t > \frac{\log\left(\epsilon / d_S(\boldsymbol{X})\right)}{\log \tau\lambda}.$$

This finishes the proof of Theorem 4. □

A.2 Observations

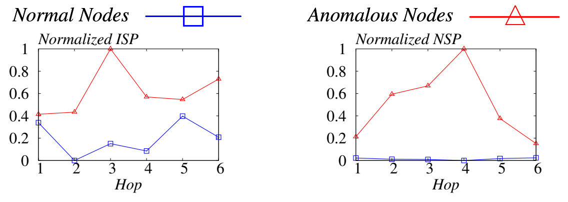

(a) Individual Smoothing Patterns (b) Neighborhood Smoothing Patterns

Figure 4: Smoothing Patterns of Reddit.

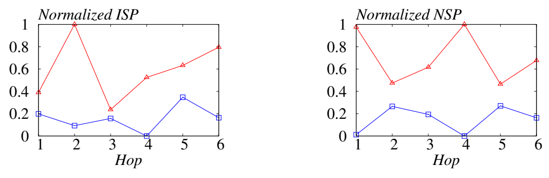

(a) Individual Smoothing Patterns (b) Neighborhood Smoothing Patterns

Figure 5: Smoothing Patterns of Tolokers.

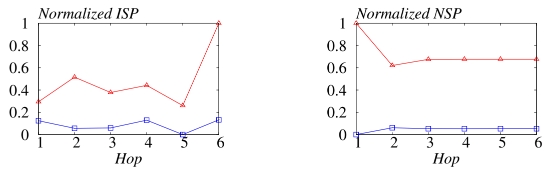

(a) Individual Smoothing Patterns (b) Neighborhood Smoothing Patterns

Figure 6: Smoothing Patterns of YelpChi.

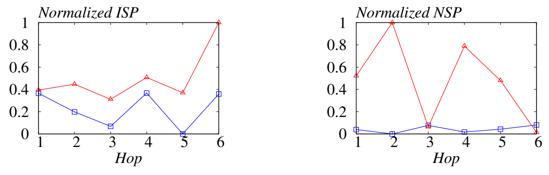

(a) Individual Smoothing Patterns (b) Neighborhood Smoothing Patterns

Figure 7: Smoothing Patterns of Questions.

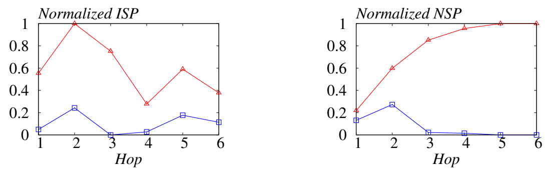

(a) Individual Smoothing Patterns (b) Neighborhood Smoothing Patterns

Figure 8: Smoothing Patterns of Elliptic.

Observations from additional datasets in Figures 4-10 further reinforce our findings. It clearly shows that the smoothing patterns of anomalous and normal nodes exhibit distinct trends and scales, where the ISP and NSP of anomalous nodes surpass those of normal nodes in most cases. Our theoretical analysis and experimental results indicate that SmoothGNN is capable of detecting even subtle differences in these smoothing patterns. This sensitivity to nuanced smoothness characteristics is the key strength of SmoothGNN.

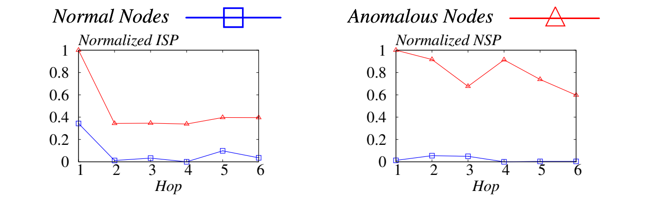

(a) Individual Smoothing Patterns (b) Neighborhood Smoothing Patterns

Figure 9: Smoothing Patterns of DGraph-Fin.

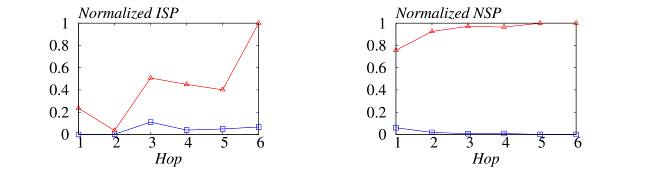

(a) Individual Smoothing Patterns (b) Neighborhood Smoothing Patterns

Figure 10: Smoothing Patterns of T-Social.

A.3 Algorithm

The detailed preprocess procedure is shown in Algorithm 1. Specifically, to facilitate the preprocess of large-scale graphs, we first apply an approximation technique to calculate the converged status of the propagation matrix, where δ represents the threshold as shown in Lines 1-6. Then, in Lines 7-10, we calculate the first $(T+1)$ hops of the augmented propagation matrix to further reduce the running time cost during the training process.

Besides, the detailed training process is shown in Algorithm 2. We use the trained model of the final epoch to conduct inference. The loss function is calculated using $\boldsymbol{H}^{SCSLC}$ and $\boldsymbol{H}^{SCGNN}$, and the anomaly score is calculated for each node using $f_{smooth}(\cdot)$ as shown in Section 4.5. To be specific, in Lines 1-2, we calculate $(T+1)$ transformations of node representations using a set of $(T+1)$ MLPs. In Line 3, the SC is encoded into $\boldsymbol{\alpha}$ as shown in Section 4.4. After that, in Lines 4-10, we use the SLC and SSGNN components to calculate $\boldsymbol{h}_i^{SLC}$ and $\boldsymbol{h}_i^{GNN}$ for each node i and apply the $\boldsymbol{\alpha}$ to serve as attention coefficients to rescale the learned representations. Notice that, to gain a superior reduction in terms of running time during the training process, we utilize the most simple architecture as the backbone. However, as shown in Section 4.1, we invent the framework from a distinct perspective, the smoothing pattern view, from all the previous works, which demonstrates the obvious differences between our work and previous ones. In Section 5, we conduct comprehensive experiments to prove the effectiveness and efficiency of our SmoothGNN.

A.4 Experimental Settings

The parameters in Table 6 are set based on the number of nodes in different graphs in Table 5. As we can see, the hidden dimensions remain stable for all three categories. However, the learning rate and number of propagation hops increase as the number of nodes grows. Besides, we employ approximation techniques to calculate the converged status of propagation, i.e., we only retain the values larger than the square of delta in the final matrix. For small graphs, we do not require approximation whereas for medium and large graphs, we set the delta to 4e-3. Furthermore, the weight initialization strategy varies across graph categories because the optimal starting point in the optimization process tends to differ depending on the graph characteristics. As for the experimental environment, we conduct all the experiments on CPUs to provide enough memory for previous works.

Algorithm 1: Preprocess

```
    Input: $\tilde{A}, T, m, n, \delta$
    Output: $[P^0, \cdots, P^T], [B^0, \cdots, B^T]$
1   $deg \leftarrow$ Degree($\tilde{A}$);
2   $deg \leftarrow \frac{deg}{\sqrt{2m+n}}$;
3   for $i = 1$ to $n$ do
4       if $deg_i \leq \delta$ then
5           $deg_i \leftarrow 0$;
6   $P^{\infty} \leftarrow deg \cdot deg^T$;
7   $P \leftarrow \frac{I_n}{2} + \frac{\tilde{A}}{2}$;
8   $L \leftarrow I_n - \tilde{D}^{-\frac{1}{2}}\tilde{A}\tilde{D}^{-\frac{1}{2}}$;
9   for $t = 0$ to $T$ do
10      $B^t \leftarrow P^t - P^{\infty}$;
11  Return $[P^0, \cdots, P^T], [B^0, \cdots, B^T]$;
```

Algorithm 2: SmoothGNN

```
    Input: $X, T, n, [P^0, \cdots, P^T], [B^0, \cdots, B^T]$
    Output: $H^{SCSLC}, H^{SCGNN}$
1   for $t = 0$ to $T$ do
2       $\tilde{X}_t \leftarrow \sigma(\text{MLP}(X))$;
3   $\alpha \leftarrow \sigma(\text{MLP}(\text{CAT}(SC(P^0\tilde{X}_0), \cdots, SC(P^T\tilde{X}_T))))$;
4   for $i = 0$ to $n$ do
5       $h_i^{SLC} \leftarrow \text{MLP}(\text{CAT}((B^0\tilde{X}_0)_i, \cdots, (B^T\tilde{X}_T))_i)$;
6       $h_i^{GNN} \leftarrow \text{MLP}(\text{CAT}((g(\tilde{X}_0)_0)_i, \cdots, (g(\tilde{X}_T)_T)_i)$;
7       $h_i^{SCSLC} \leftarrow h_i^{SLC} * \alpha$;
8       $h_i^{SCGNN} \leftarrow h_i^{GNN} * \alpha$;
9   $H^{SCSLC} \leftarrow [h_1^{SCSLC}, \cdots, h_n^{SCSLC}]$;
10  $H^{SCGNN} \leftarrow [h_1^{SCGNN}, \cdots, h_n^{SCGNN}]$;
11  Return $H^{SCSLC}, H^{SCGNN}$;
```

A.5 SMeasure during training

To explicitly show why SMeasure can be used for unsupervised NAD tasks, we report $\frac{S_a - S_n}{S_n}$ for each 10 epoch, where S_n and S_a are SMeasures of normal and anomalous nodes separately. As observed from Table 7, $\frac{S_a - S_n}{S_n}$ grows to a positive number, which means S_a is larger and grows faster than S_n as the training continues. These results tell us our framework can effectively capture the ISP and NSP through SMeasure and utilize the novel measure to effectively detect anomalous nodes.

Table 5: Statics of 9 real-world datasets.

Categories	Datasets	#Nodes	#Edges	#Feature per node	Avg. Degree	Ratio of anomalous labels
	Reddit	10,984	168,016	64	15.30	3.33%
Small	Tolokers	11,758	519,000	10	44.14	21.82%
	Amazon	11,944	4,398,392	25	368.25	6.87%
	T-Finance	39,357	21,222,543	10	539.23	4.58%
Medium	YelpChi	45,954	3,846,979	32	83.71	14.53%
	Questions	48,921	153,540	301	3.14	2.98%
	Elliptic	203,769	234,355	167	1.15	9.76%
Large	DGraph-Fin	3,700,550	4,300,999	17	1.16	1.27%
	T-Social	5,781,065	73,105,508	10	12.65	3.01%

Table 6: Parameters for SmoothGNN according to different categories.

Categories	Learning Rate	Hop	Weight Initialization	Delta	Hidden Dimensions
Small	1e-4	4	0.05	0	64
Medium	5e-4	5	0.01	4e-3	64
Large	5e-4	6	0.05	4e-3	64

Table 7: $\frac{S_a - S_n}{S_n}$ for each 10 epoch, where S_n and S_a are the SMeasures of normal and anomalous nodes separately.

Datasets	0	10	20	30	40	50	60	70	80	90	100
Reddit	0.0029	0.0410	0.0835	0.1000	0.1059	0.1105	0.1154	0.1193	0.1220	0.1237	0.1242
Tolokers	0.0722	0.2290	0.2883	0.2728	0.2704	0.2708	0.2665	0.2628	0.2631	0.2666	0.2719
Amazon	-0.0461	0.0516	0.0923	0.0892	0.1160	0.1251	0.1260	0.1288	0.1325	0.1383	0.1460
T-Finance	-0.0496	0.0004	0.0419	0.0858	0.1130	0.1253	0.1260	0.1234	0.1252	0.1254	0.1238
YelpChi	0.0353	0.0952	0.1049	0.1124	0.1140	0.1142	0.1122	0.1117	0.1103	0.1088	0.1073
Questions	0.0267	0.1211	0.1683	0.1822	0.2096	0.2351	0.2511	0.2650	0.2776	0.2915	0.3012
Elliptic	0.0036	0.1675	0.2300	0.2657	0.2858	0.2972	0.3038	0.3072	0.3084	0.3079	0.3059
DGraph-Fin	-0.0727	0.1516	0.1519	0.1518	0.1511	0.1506	0.1500	0.1496	0.1491	0.1485	0.1474
T-Social	-0.0026	0.0812	0.4438	0.4993	0.5765	0.6491	0.6986	0.7134	0.6800	0.6131	0.5334

Table 8: Additional experiments. The best result on each dataset is highlighted in boldface.

Datasets	Reddit		Tolokers		Amazon		T-Finance		YelpChi		Questions		Elliptic		DGraph-Fin		T-Social	
Metrics	AUC	AP	AUC	AP	AUC	AP	AUC	AP	AUC	AP	AUC	AP	AUC	AP	AUC	AP	AUC	AP
SmoothGNN	0.5946	0.0438	0.6870	0.3517	0.8408	0.3953	0.7556	0.1408	0.5758	0.1823	0.6444	0.0592	**0.5729**	**0.1161**	**0.6499**	**0.0199**	0.7034	0.0631
SmoothGNN-L	**0.6034**	**0.0582**	**0.7016**	**0.3670**	**0.8420**	**0.4291**	**0.7786**	**0.1514**	**0.5911**	**0.1826**	**0.6467**	0.0588	0.5670	0.1123	0.6126	0.0168	**0.7109**	**0.0711**
ONE	0.4878	0.0330	0.5041	0.2250	0.4247	0.0545	0.4311	0.0368	0.4985	0.1453	0.4995	0.0297	-	-	-	-	-	-
AdONE	0.5007	0.0322	0.5162	0.2904	0.2910	0.0444	0.6346	0.0654	0.5029	0.1513	0.6293	**0.0652**	-	-	-	-	-	-
DONE	0.5774	0.0411	0.5551	0.2877	0.3181	0.0463	0.6336	0.0647	0.5189	0.1529	0.6440	0.0646	-	-	-	-	-	-

A.6 Time Complexity Analysis

As shown in Appendix A.3, we adopt the decoupling method to precompute the propagation process, eliminating the need for calculating it at each epoch. This results in a time complexity of $O(nd_1d_2)$ per layer for SmoothGNN, where n is the number of nodes, and d_1 and d_2 are input and output dimensions of the MLP, respectively. In contrast, models that require computing the propagation process typically have a time complexity of $O(n^2d_3)$ or $O(md_3)$ per layer, where m is the number of edges, and d_3 is the embedding dimension. Notably, with $d_1, d_2 \ll n$ and $n \ll m$, SmoothGNN is more efficient in the training phase. Additionally, the time complexity for calculating the loss function in SmoothGNN is $O(nd)$, where d is the feature dimension, significantly more efficient compared to prominent baselines such as TAM with a loss function complexity of up to $O(n^2)$, given that $d \ll n$. In summary, both theoretically and empirically, SmoothGNN stands out as a highly efficient model.

A.7 Additional Experiments

To further demonstrate the effectiveness of SmoothGNN, we conduct additional experiments. Specifically, we include 3 non-GNN-based baselines, ONE [3], adONE [2], DONE [2], and a variant of our SmoothGNN called SmoothGNN-L, which applies Smoothing-aware Coefficients to all the layers of SmoothGNN. The results are shown in Table 8. Note that "-" indicates that the method failed due to memory constraints. As we can observe, our SmoothGNN can still outperform three new non-GNN-based baselines by a large margin on almost all the datasets. We can also observe that applying NSP across all the layers can lead to performance improvement on certain datasets, but not universally across all datasets. Such results demonstrate the effectiveness of NSP, as applying it solely to the final layer or throughout all layers notably outperforms baselines. Consequently, for the sake of maintaining the simplicity and stability of our model, we only apply NSP to the final layer.